Received: 31 October 2023 | Accepted: 28 February 2024

DOI: 10.1111/1462-2920.16608

BRIEF REPORT

ENVIRONMENTAL MICROBIOLOGY

Phototrophic Fe(II) oxidation by *Rhodopseudomonas palustris* TIE-1 in organic and Fe(II)-rich conditions

Verena Nikeleit[1] | **Markus Maisch**[1] | **James M. Byrne**[2] | **Caroline Harwood**[3] | **Andreas Kappler**[1,4] | **Casey Bryce**[2]

[1]Department of Geoscience, University of Tübingen, Tübingen, Germany

[2]School of Earth Sciences, University of Bristol, Bristol, UK

[3]Department of Microbiology, University of Washington, Seattle, Washington, USA

[4]Cluster of Excellence: EXC 2124: Controlling Microbes to Fight Infections, Tübingen, Germany

Correspondence
Casey Bryce, School of Earth Science, Wills Memorial Building, University of Bristol, Queens Road, Bristol BS8 1RJ, UK.
Email: casey.bryce@bristol.ac.uk

Funding information
UK Research and Innovation, Grant/Award Number: MR/V023918/1; Deutsche Forschungsgemeinschaft, Grant/Award Numbers: BR 5927/2-1, BY 82/4-1; Tübingen Structural Microscopy Core Facility (funded by the Excellence Strategy of the German Federal and State Governments)

Abstract

Rhodopseudomonas palustris TIE-1 grows photoautotrophically with Fe(II) as an electron donor and photoheterotrophically with a variety of organic substrates. However, it is unclear whether *R. palustris* TIE-1 conducts Fe(II) oxidation in conditions where organic substrates and Fe(II) are available simultaneously. In addition, the effect of organic co-substrates on Fe(II) oxidation rates or the identity of Fe(III) minerals formed is unknown. We incubated *R. palustris* TIE-1 with 2 mM Fe(II), amended with 0.6 mM organic co-substrate, and in the presence/absence of CO_2. We found that in the absence of CO_2, only the organic co-substrates acetate, lactate and pyruvate, but not Fe(II), were consumed. When CO_2 was present, Fe(II) and all organic substrates were consumed. Acetate, butyrate and pyruvate were consumed before Fe(II) oxidation commenced, whereas lactate and glucose were consumed at the same time as Fe(II) oxidation proceeded. Lactate, pyruvate and glucose increased the Fe(II) oxidation rate significantly (by up to threefold in the case of lactate). ^{57}Fe Mössbauer spectroscopy revealed that short-range ordered Fe(III) oxyhydroxides were formed under all conditions. This study demonstrates phototrophic Fe(II) oxidation proceeds even in the presence of organic compounds, and that the simultaneous oxidation of organic substrates can stimulate Fe(II) oxidation.

INTRODUCTION

Iron (Fe), an important redox-active element in the environment, interacts with major nutrient cycles, including carbon, nitrogen and sulphur, and affects the bioavailability and fate of toxic metals, pollutants and nutrients (Eickhoff et al., 2014; Kappler et al., 2021; Mu et al., 2016; Tipping, 1981). Some anoxygenic phototrophs can oxidise Fe(II) (photoferrotrophs) and are widespread in various environments and throughout Earth's history (Ehrenreich & Widdel, 1994; Heising et al., 1999; Jiao et al., 2005; Kappler et al., 2005; Laufer et al., 2017; Llirós et al., 2015; Straub et al., 1999). The surface of Earth's ancient oceans was an ideal habitat for these bacteria, with high concentrations of dissolved Fe(II) (up to 0.5 mM), the presence of light, and anoxic conditions (Poulton & Canfield, 2011). During that time, vast Fe(III)-rich deposits were formed, known as banded iron formations (BIFs), and it is thought that photoferrotrophs could have played a key role in their formation (Kappler et al., 2005; Konhauser et al., 2002; Thompson et al., 2019). Although conditions on Earth today are not as favourable for photoferrotrophs given the ubiquity of oxygen, there are still habitats where they can thrive, in sweet spots where anoxic conditions, light and dissolved Fe(II) are present simultaneously, such as stratified lakes, freshwater and marine sediments and small iron-rich ponds (Crowe et al., 2017; Heising et al., 1999; Jiao et al., 2005; Laufer et al., 2017).

A number of strains isolated from the groups of green sulphur, purple sulphur, and purple non-sulphur

bacteria have given insights into the metabolism of photoferrotrophs. These include four green sulphur bacteria: *Chlorobium ferrooxidans* KoFox (freshwater co-culture, Heising et al., 1999), *Chlorobium* sp. N1 (marine co-culture, Laufer et al., 2017), *Candidatus* Chlorobium masyuteum (freshwater, co-culture, Lambrecht et al., 2021) and *Chlorobium* phaeoferrooxidans KB01 (first pure isolate, sourced from a stratified lake; Crowe et al., 2017). For the purple non-sulphur bacteria, *Rhodobacter ferrooxidans* SW2 and *Rhodopseudomonas palustris* TIE-1 are used as models for freshwater strains and have been extensively studied (Bird et al., 2011; Ehrenreich & Widdel, 1994; Jiao et al., 2005; Kappler & Newman, 2004; Miot et al., 2009). *R. ferrooxidans* SW2 was isolated from a freshwater sediment and *R. palustris* TIE-1 from a marsh sediment. *Rhodovulum iodosum* and *Rhodovulum robiginosum* are representatives of marine purple non-sulphur strains and from purple sulphur bacteria *Thiodictyon* sp. F4 is used as a model strain (Croal et al., 2004; Straub et al., 1999).

Although these microbes were mostly studied with regards to their ability to oxidise Fe(II), they are metabolically flexible and can grow photoheterotrophically and photoautotrophically with a variety of substrates as electron donors (Jiao et al., 2005; Laufer et al., 2017). When grown photoautotrophically these organisms fix CO_2 to build biomass while using different inorganic substrates (H_2, H_2S, $S_2O_3^{2-}$ or Fe(II)) as an electron source (Figure 1). For photoheterotrophic growth, they can use a wide range of organic substrates like acetate, lactate and pyruvate, as well as larger molecules like glucose. These organic compounds can be used as a carbon source to build biomass or/and as an electron donor (Figure 1). McKinlay and Harwood (2010) found that 22% of acetate used by *R. palustris* was oxidised to CO_2 and used to recycle cofactors necessary for building biomass. Therefore, CO_2 plays an important role for these phototrophs as a carbon source and as a way to recycle cofactors (McKinlay & Harwood, 2010). Further studies investigated how these bacteria would behave when they have multiple substrates present, as they can grow photoautotrophically and photoheterotrophically (Figure 1).

Ehrenreich and Widdel (1994) found that organics (glucose and acetate) were used before Fe(II) was oxidised by *R. ferrooxidans* SW2, but *Chromatium* L7 used the substrates at the same time. Several years later, Melton et al. (2014) studied whether *R. palustris* TIE-1 can oxidise Fe(II) in the presence of acetate and lactate. However, in that study, relatively high substrate concentrations were used (5 mM Fe(II); 20 mM acetate and lactate) and different consumption scenarios were observed. In the case of acetate and Fe(II), acetate was consumed first, followed by Fe(II) oxidation, whereas with lactate and Fe(II), both substrates were used simultaneously. So far, no study has explicitly investigated the effect of utilisation of co-substrates on Fe(II) oxidation, especially the effect of organic co-substrates on Fe(II) oxidation rates and mineral formation at environmentally relevant substrate concentrations.

As organic compounds are ubiquitous in the environment and also play an important role for photoferrotrophs, we investigated how different organic substrates and CO_2 availability influence the oxidation of Fe(II) by the photoferrotrophic strain *R. palustris* TIE-1, as well as how the presence of organics influences the identity of the minerals that formed during Fe(II) oxidation. A wide range of organic substrates were tested, including easily accessible organic compounds such as acetate, lactate and pyruvate. Butyrate was tested as an example of a more reduced carbon substrate and glucose as a more complex organic substrate. In addition, to assess the importance and role of CO_2 in co-substrate utilisation, experiments were

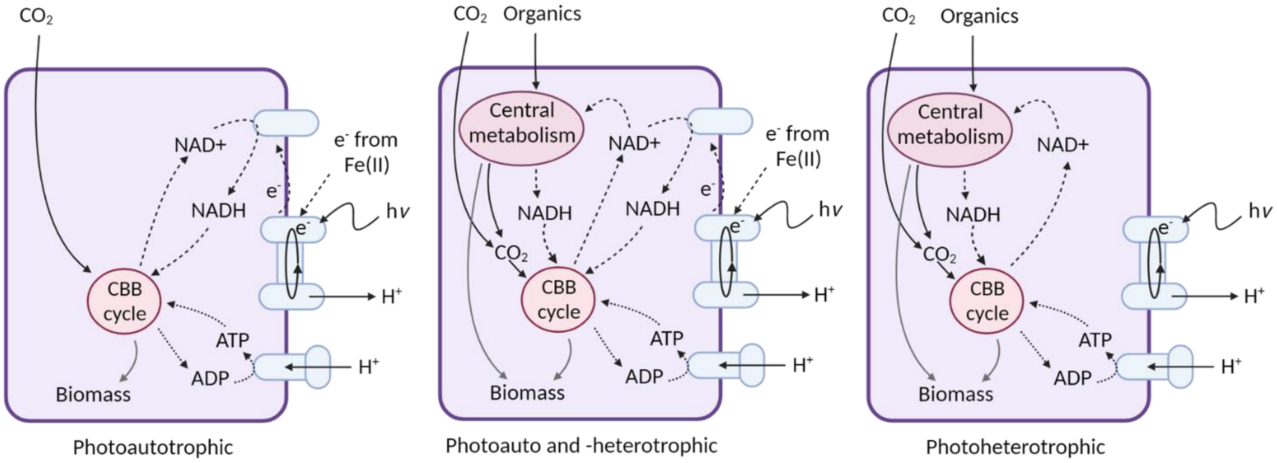

FIGURE 1 Schematics of photoautotrophic (left), mix of photoauto- and heterotrophic (middle), and heterotrophic growth (right) of *Rhodopseudomonas palustris* TIE-1. Created with BioRender.

conducted both in the presence and absence of CO_2/HCO_3.

EXPERIMENTAL PROCEDURES

Effects of organic substrates on Fe(II) oxidation

For substrate preference experiments *R. palustris* TIE-1, a well-studied photoferrotrophic strain, was chosen (Jiao et al., 2005). *R. palustris* TIE-1 was grown for two transfers on H_2/CO_2 (80:20; vol:vol) before the experiment to avoid bias towards any of the experimental substrates. 50 mL of media was added to 100 mL serum vials and inoculated with 0.5% of the pre-grown *R. palustris* TIE-1 culture. Media was prepared as stated in Jiao et al. (2005). The following salts were dissolved in 1 L of ultrapure water: 0.5 g KH_2PO_4, 0.3 g NH_4Cl, 0.5 g $MgSO_4 \cdot 7H_2O$, 0.1 g $CaCl_2 \cdot 2H_2O$ and autoclaved in a Widdel flask. After autoclaving, 10 mL/L filter-sterilised vitamin solution (altered from Ehrenreich & Widdel, 1994; containing 50 mg/L riboflavin), 1 mL/L SL10 trace element solution (Widdel, 1983), 1 mL/L selenite-tungstate solution (Widdel & Bak, 1992) and 0.1 mg/L vitamin B12 solution were added. The medium was prepared with a headspace of N_2/CO_2 (90:10; vol:vol) and buffered with 22 mM HCO_3^-. The pH of the media was adjusted to pH 7 with anoxic 1 M HCl and anoxic 0.5 mM H_2CO_3.

For the substrate preference experiments, three different setups were used. In the first setup, only $FeCl_2$ was added. In the second setup, $FeCl_2$ and an organic substrate (0.6 mM) (either acetate [Ac], lactate [Lc], pyruvate [Py], butyrate [Bu] or glucose [Glu]) were added. In the third setup, only organic substrates (0.6 mM) were added. For the setups with Fe(II), 4.5 mM $FeCl_2$ was added to the medium and left for 48 h at 4°C to allow precipitation of Fe(II) minerals before the medium was filtered (0.22 μm) in an anoxic glovebox (100% N_2). This led to a starting concentration of approximately 2 mM dissolved Fe(II) in the experimental setups. The concentrations used are the minimum required to be able to track substrate consumption by our analytical methods. Although they are on the higher side of those found in the environment, they are environmentally relevant. For example, they are similar to those found in some wetlands, for example, by Patzner et al. (2020). The organic compounds were added after the filtration step. Four replicate bottles were inoculated in the setups with Fe(II), with one used as a sacrificial bottle for mineral analysis by Fe^{57}-specific Mössbauer spectroscopy - this bottle was sampled only at the end of the incubation. For abiotic controls, two bottles per substrate and setup were used without adding any bacteria. Abiotic controls were set up to evaluate any adsorption of Fe(II) to the glass wall and to ensure the absence of abiotic reactions between Fe and the chosen organic substrate. In the three biotic bottles, continuous sampling and analysis of Fe, cell numbers and organics were performed. The abiotic bottles were sampled and analysed at a subset of these time points for concentrations of Fe and organics. Samples were taken anoxically and under sterile conditions at the bench and samples for mineral analysis were taken in an anoxic glovebox (100% N_2). During the experiments, the vials were placed in a light incubator with 25 ± 7 μmol photons/s/m^2 at 20°C and positioned randomly on the shelf to avoid biases based on position in the incubator. The Fe(II)-only setup was repeated with four bottles and all data show an average of four bottles. In the setup of Fe(II) plus butyrate, only two bottles showed Fe(II) oxidation, and in the glucose-only setup only two bottles showed glucose consumption.

Fe(II) oxidation experiments in PIPES-buffered medium lacking CO_2

CO_2 is essential for autotrophic Fe(II) oxidation. Therefore, we tested whether Fe(II) could also be oxidised by *R. palustris* TIE-1 in the absence of CO_2/HCO_3^- when *R. palustris* TIE-1 utilises different organic substrates in parallel to Fe(II). This experiment had the same conditions as the substrate preference experiment described above except that 20 mM piperazine-*N*,*N*′-bis(2-ethanesulfonic acid) (PIPES) was chosen as a buffer and the headspace contained only N_2. For this experiment, *R. palustris* TIE-1 was also pre-grown on H_2/CO_2 (80:20; vol:vol) for two consecutive transfers in bicarbonate-buffered media. The pre-culture cells were washed twice before inoculation to remove any residual bicarbonate from the inoculum. For this, serum vials were centrifuged at 5000 rpm for 5 min anoxically. The supernatant was then exchanged with a syringe to keep the serum vial anoxic and replaced with 20 mM PIPES buffer.

Fe quantification

Fe(II) and Fe(III) were quantified spectrophotometrically with a modified ferrozine assay (Hegler et al., 2008). During sampling, 0.1 mL of sample was added to 0.9 mL of 1 M HCl. Samples were stored at 4°C until analysis. The ferrozine-Fe(II) complex was quantified at 562 nm using a microtiter plate reader (Thermo Scientific Multiscan, Thermo Fisher Scientific). Ferrozine measurements were conducted in triplicates. All rates were calculated over at least three data points.

Short-chain fatty acid analysis

High-performance liquid chromatography (HPLC) analysis was performed with a Shimadzu Prominence

HPLC with an LC-20ATsolvent delivery unit, a CTO-10ASvp column oven, and a RID-20a refractive index detector. After sampling, samples were centrifuged at 15,000 rpm for 10 min to remove cells and minerals, and the supernatant was transferred to a new Eppendorf tube and stored at 4°C until analysis.

Cell number quantification

Samples (1.8 mL) were stored at −20°C for DNA extraction and qPCR of 16S rRNA. DNA was extracted using the UltraClean R Microbial DNA Isolation Kit (MO BIO Laboratories, Carlsbad, CA, USA) and the quantity of the DNA was measured with a NanoDrop ND-1000 Spectrometer (NanoDrop™ 1000; Thermo Scientific, Waltham, MA, USA). qPCR was conducted with the iCycler iQ™Real-Time PCR Detection System and the Bio-Rad CFX Maestro 1.1 software. 16S rRNA was quantified with the 341F (CCTACGGGAGGCAGCAG) and 797R (GGACTACCAGGGTATCTAATCCTGTT) primer pair (Nadkarni et al., 2002). A mix of 5 μL SYBR green, 0.15 μL 341F primer, 0.45 μL 797R primer, 3.4 μL H_2O and 1 μL of sample was prepared for the number of samples, standards and negative control in triplicates with a reaction volume of 10 μL. For standards, plasmids with respective genes were used and quantified with Qubit 2.0 (Invitrogen, Carlsbad, CA, USA).

Statistical analysis

To evaluate if differences between conditions were statistically significant, we performed Welsh's *t*-test to account for unequal variances between each sample treatment. We chose a significance threshold of $\alpha = 0.05$.

Mineral analysis by Mössbauer spectroscopy

Within an anoxic glovebox (100% N_2), 20 mL liquid sample was collected from each microcosm, filtered through a 0.45 μm pore space syringe filter (area 1 cm^2), and covered with Kapton tape, forming a thin disc. Samples were stored under anoxic conditions at −18°C to avoid microbial activity and mineral transformation. Individual samples were transported to the Mössbauer instrument within airtight bottles, which were only opened immediately before loading into a closed-cycle exchange gas cryostat (Janis Cryogenics) under a backflow of He to minimise exposure to air. Spectra were collected at 77 K using a constant acceleration drive system (WissEL) in transmission mode with a ^{57}Co/Rh source. All spectra were calibrated against a 7 μm thick α-^{57}Fe foil that was measured at room temperature. Analysis was carried out using Recoil (University of Ottawa) and the Voigt Based Fitting routine (Rancourt & Ping, 1991). The half-width at half maximum was constrained to 0.134 mm/s during fitting.

Scanning electron microscopy

Scanning electron microscopy (SEM) was conducted to visualise the interactions and associations between the microbial cells and the minerals. For SEM, cultures of *R. palustris* TIE-1 were grown with Fe(II) only, Fe(II) plus acetate, Fe(II) plus lactate and Fe(II) plus glucose. At the end of the incubation, a sample was fixed by adding glutaraldehyde (2.5%; vol/vol). 30 μL of fixed samples were placed on a glass slide, which was coated with 50 μL of poly-L-lysine. The samples were dehydrated with increasing ethanol solutions starting from 35% to 100% (5 min per new solution; 35%, 55%, 70%, 90% to 100%). The samples were then placed in HMDS two times for 30 s and left in the fume hood to dry. Samples were placed on aluminium stubs and sputter-coated at a working distance of 35 mm at 20 mA for 70 s to receive a 13 nm coating (BAL-TEC SCD 005). Microscopy was done with a ZEISS Crossbeam 550 L using an electron high tension of 2 kV, a working distance of 1.5 mm, and a secondary electron secondary ion detector.

RESULTS AND DISCUSSION

R. palustris TIE-1 substrate preferences

To determine the effect of organic substrates on Fe(II) oxidation, *R. palustris* TIE-1 was grown in CO_2/HCO_3^- buffered media with Fe(II) only, Fe plus an organic substrate (acetate, lactate, pyruvate, butyrate or glucose) or organics alone. We found that *R. palustris* TIE-1 consumed all of the added organics completely and oxidised Fe(II). Both sequential and simultaneous consumption of organics alongside Fe(II) oxidation was observed during the experiment, depending on the identity of the organic compound. In the abiotic setup, no changes in organic substrate and Fe(II) concentrations were observed (data not shown). In the setups with Fe(II) plus acetate (Ac), Fe(II) plus pyruvate (Py) and Fe(II) plus butyrate (Bu), the organics were consumed first, followed by the oxidation of Fe(II) (Figure 2B,D,F). No lag phases in the consumption of these organics were observed and were consumed within 3.3 days (Ac plus Fe(II)) to 4 days (Bu and Py plus Fe(II)) (Figure 2B,D,F), respectively. Once the organics were consumed, Fe(II) was oxidised to an extent of 84 ± 5% (with acetate), 90 ± 2% (with pyruvate) and 84 ± 3% (with butyrate). In the setups

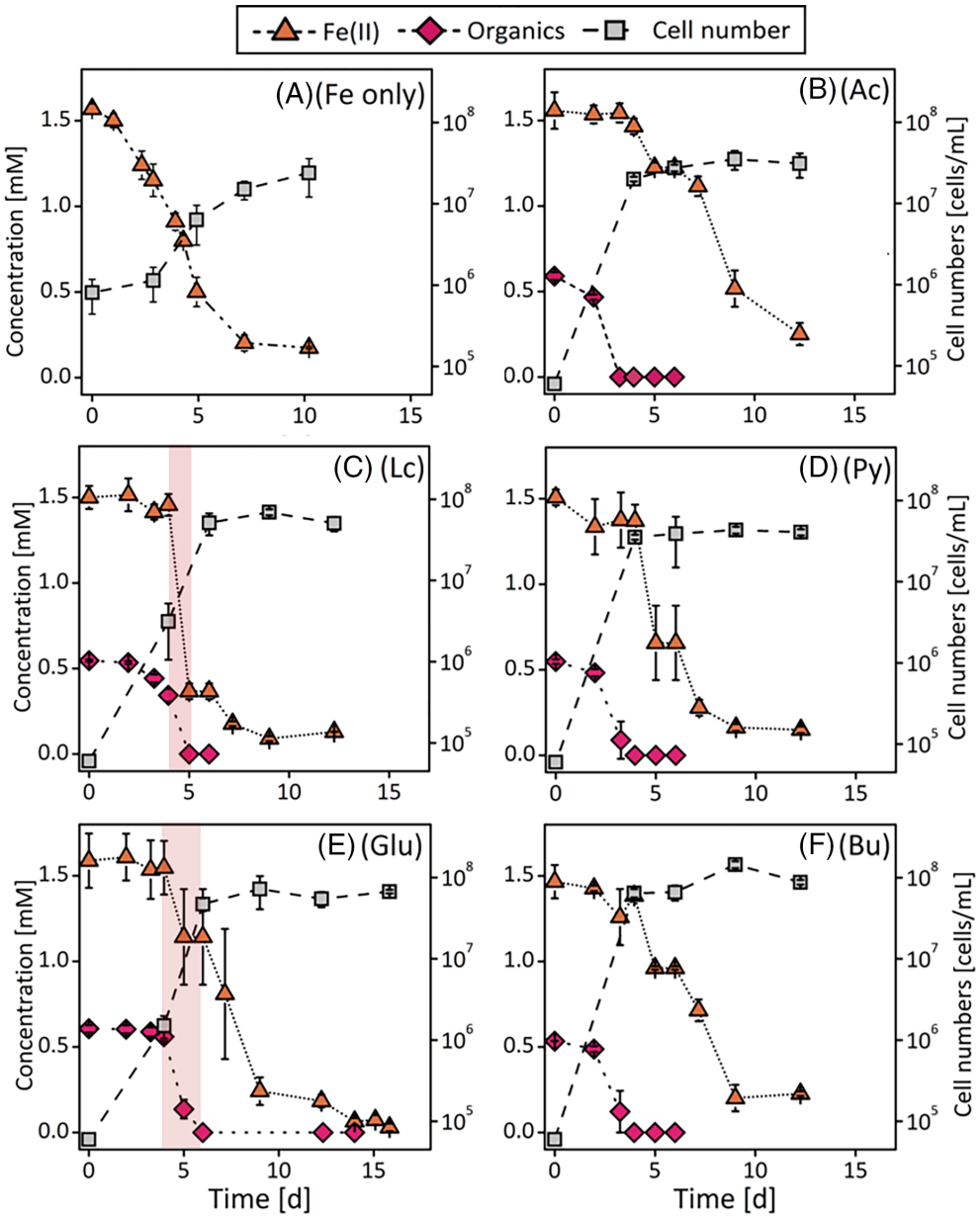

FIGURE 2 Growth of *Rhodopseudomonas palustris* TIE-1 with different growth substrates. (A) *R. palustris* TIE-1 grown only with Fe(II). (B–F) *R. palustris* TIE-1 was grown with Fe(II) plus an organic substrate (either acetate (B-Ac), lactate (C-Lc), pyruvate (D-Py), butyrate (E-Bu) or glucose (F-Glu)). The standard deviation is based on biological triplicates, in case of A standard deviation is based on four bottles. The pink background shows simultaneous consumption of an organic substrate and Fe(II). All media were buffered with CO_2/HCO_3.

with Fe(II) plus lactate and Fe(II) plus glucose, Fe(II) oxidation reached 91 ± 1% and 98 ± 2%, respectively. In the latter two cases, simultaneous consumption of Fe(II) and organics was observed (Figure 2C,E). In the case of Fe(II) only, 89% of Fe(II) was oxidised (Figure 2A). Our data expanded our understanding of different substrate preferences for *R. palustris* TIE-1 and were determined for the first time for pyruvate, butyrate, and glucose. We could also show that the findings of Melton et al. (2014) regarding the substrate preference of acetate, lactate and Fe(II) hold true even at much lower, environmentally relevant substrate concentrations.

However, in their study, substrate concentrations were many folds higher (16 mM organic compounds and 5 mM Fe(II)). Our results, in combination with theirs, demonstrate that consumption order is independent of substrate concentrations. In addition, the substrate preferences of strain *R. palustris* TIE-1 appear to differ from those of other photoferrotrophs. Ehrenreich and Widdel showed that *R. ferrooxidans* SW2 used these substrates in a sequential order (acetate and glucose before Fe(II); Ehrenreich & Widdel, 1994). In the same study, a second strain, *Chromatium* L7, was shown to consume the organics (glucose or acetate) and Fe(II) at the same time (Ehrenreich &

Widdel, 1994). This contrasts with our findings where *R. palustris* TIE-1 used glucose and Fe(II) at the same time but used acetate before Fe(II). These studies suggest that substrate preferences are independent of substrate concentrations but are likely unique to individual strains of phototrophic Fe(II) oxidisers. These results regarding the substrate preference of *R. palustris* TIE-1 help us to understand how different photoferrotrophs could actively contribute to Fe(II) oxidation under various conditions and show that in the environment, Fe(II) will still be oxidised even when these cells have the option to conduct photoheterotrophy (arguably a more favourable metabolism).

Effect of multiple substrates on consumption rates of both organics and Fe(II)

Fe(II) and organics each influenced the consumption rate of the other substrates. For the setup with Fe(II) only, in a bicarbonate-buffered medium, Fe(II) oxidation was completed for all four bottles after 10.2 days with an average Fe(II) oxidation rate of 0.23 ± 0.04 mM/day (Figure 3A). This Fe(II) oxidation rate corresponds well to previously published data for the same strain (0.27 ± 0.01 mM/day [Han et al., 2020] and 0.15 ± 0.03 mM/day [Peng et al., 2019]) which also measured Fe(II) oxidation rates in the absence of alternative substrates. Fe(II) oxidation rates for setups with Fe(II) plus butyrate (0.24 ± 0.01 mM/day) were in the same range as in the setup with Fe(II) only. With acetate, the Fe(II) oxidation rate was slightly lower (0.17 ± 0.01 mM/day) than with Fe(II) alone. For the setups with Fe(II) plus pyruvate (0.34 ± 0.02 mM/day), Fe(II) plus glucose (0.33 ± 0.04 mM/day) and Fe(II) plus lactate (1.05 ± 0.02 mM/day), Fe(II) oxidation rates were significantly increased and in the case of Fe(II) plus lactate, increased more than threefold (Table A1). We also observed that Fe(II) affected the consumption rates of organic compounds (Figure 3B). For lactate (with Fe(II) 0.25 ± 0.01 mM/day and without Fe(II) 0.21 ± 0.02 mM/day), butyrate (with Fe(II) 0.31 ± 0.06 mM/day and without Fe(II) 0.17 ± 0.002 mM/day) and glucose (with Fe(II) 0.27 ± 0.01 mM/day and without Fe(II) 0.12 ± 0.03 mM/day), the consumption of the organics was enhanced when Fe(II) was present. For lactate, this increase was statistically significant (Table A1). For glucose and butyrate consumption, the addition of Fe(II) had a large beneficial impact and increased consumption rates 1.7-fold for butyrate and 2-fold for glucose. In the case of acetate and pyruvate, consumption rates with and without Fe(II) were within the error range (acetate: with Fe(II) 0.18 ± 0.01 mM/day

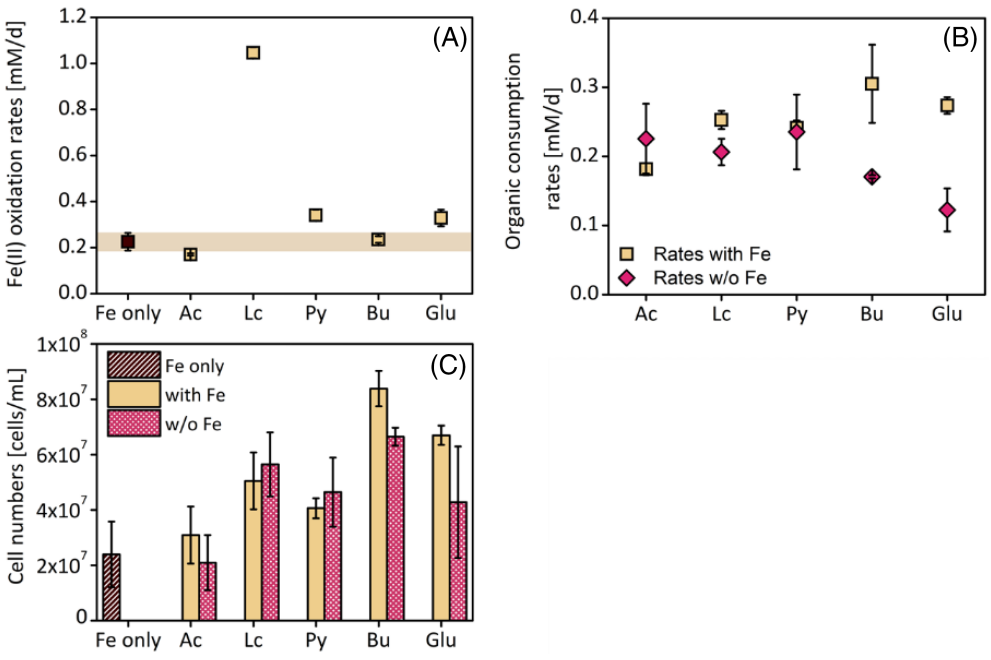

FIGURE 3 (A) The Fe(II) oxidation rates of *Rhodopseudomonas palustris* TIE-1 incubated with acetate (Ac), lactate (Lc), pyruvate (Py), butyrate (Bu) or glucose (Glu). The dark brown point shows the Fe(II) oxidation rate when only Fe(II) was added and the light brown background shows the standard deviation. Significant differences in Fe(II) oxidation rates were calculated with lactate, pyruvate and glucose (Table A1). (B) The organic consumption rates when the organics and Fe(II) were added together (light brown square) or when only the organics were added (pink diamond). Significant differences with organic consumption rates were calculated with lactate (Table A1). (C) Cell numbers of *R. palustris* TIE-1 at the end of the experiment for Fe(II) only (dark brown), organics plus Fe(II) (light brown) and only organics (pink with pattern). For Fe plus butyrate and glucose alone, only duplicates are shown and the range is calculated for Fe-only the average was calculated from four replicates. For all other setups, averages and rates were calculated from triplicates. All experiments were carried out in CO_2/HCO_3-buffered media.

and without Fe(II) 0.23 ± 0.05 mM/day; pyruvate: with Fe(II) 0.24 ± 0.01 mM/day and without Fe(II) 0.24 ± 0.05 mM/day).

In general, organic compounds with more carbon atoms tended to show lower consumption rates without Fe(II) than those with fewer carbon atoms but displayed higher consumption rates when Fe(II) was present. For Fe(II) oxidation the type of organic plays an important role in our study. Acetate and butyrate, 2 and 4 C atoms, did not influence Fe(II) oxidation, whereas 3 and 6 C atom organics (lactate, pyruvate and glucose) lead to a significant increase in Fe(II) oxidation rates. We could also observe that for some substrates, both consumption rates were increased (for glucose, lactate and Fe(II)), but in other cases, only one consumption rate would increase (Fe(II) oxidation rate with pyruvate; butyrate consumption rate with Fe(II)). This demonstrates the complexity of these interactions and shows that co-substrate utilisation can be beneficial for the consumption of both substrates. With these data, we expand our understanding of how turnover rates of both organic and inorganic substrates could be interdependent in the environment.

The observation that lactate stimulated Fe(II) oxidation by *R. palustris* TIE-1 was also made by Heising and Schink (1998) and by Melton et al. (2014); but was demonstrated at much higher substrate concentrations that favoured organic consumption. It has not previously been shown that these other substrates could also simulate Fe(II) oxidation. Heising and Schink showed for a different strain, *Rhodomicrobium vannielii* strain BS-1, that Fe(II) oxidation was stimulated by the addition of acetate or succinate, suggesting these benefits of co-substrate utilisation are likely universal across the Fe(II)-oxidising phototrophs. Co-substrate utilisation with non-organic substrates has been studied previously and, contrary to our findings with organics, found that Fe(II) oxidation rates of *R. palustris* TIE-1 and *R. ferrooxidans* SW2 decreased in the presence of H_2 and were generally higher with high (20 mM) compared to low (1 mM) $NaHCO_3$ concentrations. Our experiments suggest that contrary to what may be expected, the availability of organic compounds in the environment and, thus, the option for this strain to conduct both photoheterotrophy and photoautotrophy simultaneously may be beneficial for both metabolisms.

Another advantage of multiple substrate use is that bacteria can utilise substrates that were not bioavailable to them before. Our strain could use all of the tested substrates, however, in a study by Govindaraju et al. (2019) *R. palustris* CGA009 could not use lactate alone, but when acetate and succinate were also added, this strain could use lactate. In another study, *Rhodobacter capsulatus* SB1003 could not solely grow with Fe(II) or citrate alone. When Fe(II) and citrate were used together, Fe(II) and citrate were broken down photochemically to form acetoacetic acid that supported growth (Caiazza et al., 2007). Both substrates could also bind to each other, which makes it easier for the bacteria to use. For *R. capsulatus* SB1003 it has been shown that it could oxidise Fe(II) when it was chelated with NTA (nitrilotriacetate) (Kopf & Newman, 2012). It has also been shown for this bacteria that the humic substances bind free Fe(II) and thus alleviate the toxicity of free Fe(II) to *R. capsulatus* SB1003 (Poulain & Newman, 2009).

In summary, our experiments show that *R. palustris* TIE-1 consumes Fe(II) and different organic substrates simultaneously or sequentially and that the extent and rate of Fe(II) oxidation is influenced by the identity of the organics present and vice versa. It shows that under the right conditions, Fe(II) oxidation could be a more prominent reaction in the environment than previously thought.

Effects of different substrates on growth

In setups with acetate, pyruvate and butyrate plus Fe(II), rapid cell growth was observed and continued when Fe(II) was oxidised. Setups with lactate and glucose showed a slower initial rise in cell numbers. The second lowest cell numbers were measured in the setup with Fe(II) only (2.4 ± 1.2 × 10^7 cells/mL). In general, cell numbers in setups with Fe(II) plus organic compounds increased according to the number of carbons in the organic compound provided (i.e., butyrate > lactate > acetate) (Figure 3C). The highest cell numbers were reached with Fe(II) plus butyrate (8.4 ± 0.6 × 10^7 cells/mL) and Fe(II) plus glucose (6.7 ± 0.3 × 10^7 cells/mL). In both cases, cell numbers with Fe(II) were higher compared to cell numbers with organics alone. This was also true for Fe(II) plus acetate (with Fe(II) 3.1 ± 1.0 × 10^7 cells/mL and without Fe(II) 2.1 ± 1.0 × 10^7 cells/mL). In the cases of lactate and pyruvate, cell numbers were slightly higher without Fe(II) (lactate: with Fe(II) 5.1 ± 1.0 × 10^7 cells/mL and without Fe(II) 5.7 ± 1.2 × 10^7 cells/mL; pyruvate: with Fe(II) 4.1 ± 0.3 × 10^7 cells/mL and without Fe(II) 4.7 ± 1.3 × 10^7 cells/mL).

We also compared these counted cell numbers to numbers predicted based on the available carbon in the organic substrates (Table A2), assuming a cell weighs 1 pg (dry weight consisting of CH_2O). For the calculations for the Fe(II) only setup, we assumed all electrons are used for fixing CO_2 into biomass ($CO_2 \rightarrow CH_2O$; four electrons). Based on this calculation, the cell numbers for the setup with only Fe(II) should have been ca. 1.4 × 10^7 cells/mL, which is close to our measured number of 2.4 ± 1.2 × 10^7 cells/mL. For setups with organic substrates, a similar approach was used. McKinlay and Harwood (2010) found that in an incubation of *R. palustris* strain CGA009 and CGA010 with 20 mM of acetate, 93% of the added acetate was

converted into biomass. For simplicity, we assumed that 90% of the other organic substrates tested in our study were also converted into biomass. We would expect (1) higher cell numbers with organic compounds with more C atoms and (2) the formation of more cells when the organic compounds are used together with Fe(II) as substrates. The cell number calculations (Table A2) matched the measured cell numbers when either Fe(II) or the organic compounds were used alone. This was the case for acetate (2 C atoms), lactate/pyruvate (3 C atoms), and butyrate (4 C atoms), whereas setups with glucose (6 C atoms) showed lower cell numbers than the setups with butyrate. In the setups with lactate and pyruvate, the addition of Fe(II) did result in higher cell numbers, as expected from theoretical calculations. This demonstrates that the addition of Fe(II) or substances with more C atoms does not necessarily lead to an increase in cell number.

Influence of organics on mineral identity and morphology of cell-mineral aggregates formed during Fe(II) oxidation

A consequence of microbial Fe(II) oxidation is the formation of Fe(III) minerals. Therefore, we investigated how Fe(III) minerals and their associations with cells are affected by the presence of organic co-substrates using Fe^{57} Mössbauer spectroscopy and SEM. Samples from the setups containing either Fe(II) plus acetate, Fe(II) plus lactate, Fe(II) plus butyrate and Fe(II) plus pyruvate were collected after 12.3 days and samples from setups containing Fe(II) only and Fe(II) plus glucose were harvested after 15.8 days. Fe^{57} Mössbauer spectroscopy analyses of all samples at 77 K showed short-range ordered Fe(III) oxyhydroxide minerals, likely ferrihydrite, as the dominant mineral phase (Figure A4). The only difference between the minerals collected from the different setups was the relative abundance of the remaining Fe(II) compared to the formed Fe(III) mineral. Setups with Fe(II) plus lactate showed the lowest abundance of remaining Fe(II) mineral phases (6%), whereas 94% of all iron mineral phases were present as poorly crystalline Fe(III) oxyhydroxides (Table A3). Setups with either Fe(II) only, Fe(II) plus pyruvate or Fe(II) plus butyrate showed similar abundances of remaining Fe(II) minerals of around 15% plus 85% ferrihydrite. The highest abundance of remaining Fe(II) mineral phases was detected in samples containing Fe(II) plus acetate (32%) and Fe(II) plus glucose (40%). Our results with the organics show that *R. palustris* TIE-1 consistently forms poorly crystalline Fe(III) oxyhydroxides when cultivated in this media and that the presence of external organic substrates does not influence the minerals formed. This mineral phase is consistently found in studies of Fe(II) oxidation by *R. palustris* TIE-1 (e.g., Han et al., 2020) when no organics are present. This indicates that, despite the presence of organic compounds influencing the onset and rates of Fe(II) oxidation, the mineral formation is unaffected.

Although the identity of the Fe(III) minerals formed was the same for all setups (i.e. ferrihydrite), we were interested in whether there are differences in mineral surface morphology depending on the identity of the organics added as co-substrates. Therefore, SEM images were collected for the setups containing either Fe(II) only, Fe(II) plus acetate, Fe(II) plus lactate, and Fe(II) plus glucose. We found that samples from setups containing Fe(II) only showed spiky plates (Figures 4 and A5). Similar mineral morphologies were also found in setups where organic substrates were present in addition to the Fe(II). We also observed cells embedded in the minerals (Figure 4). With more carbon substrates added, more cells were seen by SEM in the samples, which is consistent with our data on cell numbers. Most of the cells were observed in the setup containing Fe(II) plus glucose. Here, the surface of the minerals was covered with cells, and web-like structures of organic matter were observed (probably EPS) (Figure 4). EPS structures in previous publications showed similar features to those we found in our SEM images (Diaz et al., 2017; Dohnalkova et al., 2011; Solmaz et al., 2018).

In summary, we observed that the presence of organic substrates in addition to Fe(II) did not affect the composition of the Fe(III) minerals formed by photoferrotrophs.

Effect of replacing CO_2/HCO_3 buffer with PIPES on Fe(II) oxidation and organic consumption

CO_2 is essential for autotrophic Fe(II) oxidation and for balancing the internal redox potential of substrates more negative than biomass (McKinlay & Harwood, 2010). To investigate the impact of CO_2 on the patterns of substrate consumption, we exchanged the bicarbonate buffer for PIPES buffer and repeated the experiments. In the absence of CO_2/HCO_3, cells grew on acetate, lactate and pyruvate, but there was no growth with butyrate and glucose (Figures 5 and A1). Growth with glucose could, however, be observed in a separate experiment (Figure A3). No Fe(II) oxidation occurred in the setup when only Fe(II) was present or when Fe(II) was present together with the organic co-substrates. However, Fe(II) did stimulate growth on lactate in a PIPES-buffered medium. Cell numbers of Fe(II) plus lactate ($3.0 \pm 1.6 \times 10^7$ cells/mL) were three times higher than without Fe(II) ($0.9 \pm 0.7 \times 10^7$ cells/mL; Figure 5A). For pyruvate, no beneficial effect was observed in the PIPES setups (with Fe(II) $1.7 \pm 0.5 \times 10^7$ and without Fe(II) $1.7 \pm 0.1 \times 10^7$ cells/mL), and in the case of acetate, cell

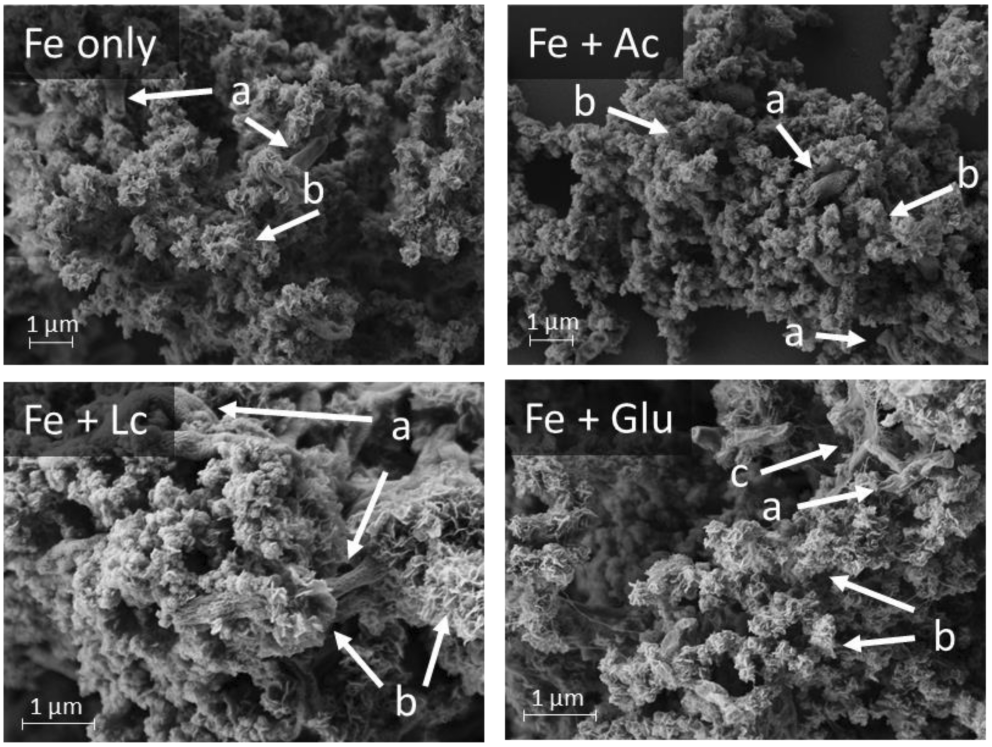

FIGURE 4 Scanning electron microscopy images of *R. palustris* TIE-1 grown with only Fe(II) (Fe-only), with Fe(II) plus acetate (Fe + Ac), with Fe(II) plus lactate (Fe + Lc) and with Fe(II) plus glucose (Fe + Glu). Arrow a shows the cells of *R. palustris* TIE-1, arrow b shows the spiky minerals and arrow c shows web-like structures.

numbers were lower (with Fe(II) $1.0 \pm 0.1 \times 10^7$ and without Fe(II) $1.6 \pm 0.3 \times 10^7$ cells/mL). When comparing cell numbers from PIPES-buffered medium setups to experiments with CO_2 /HCO_3^- buffered medium, we found that cell numbers were higher when CO_2 was present except for the setups with acetate alone (Figure 5A).

In the next step, organic consumption rates were calculated. No difference in the consumption rates for acetate was observed; these reached 0.16 ± 0.05 mM/d with Fe(II) and 0.14 ± 0.01 mM/day without Fe(II) (Figures 5B and A2). The same was also observed with lactate, although overall consumption rates were lower compared to acetate (with Fe(II) 0.10 ± 0.03 and without Fe(II) 0.12 ± 0.02 mM/day). For acetate consumption rates, values were not significantly different (with/without CO_2). However, consumption rates of lactate with CO_2 were significantly higher than without CO_2. This applied to both lactate alone and with Fe(II) (Table A1). Pyruvate concentrations and consumption rates could not be measured during the experiment due to interference of PIPES and with Pyruvate peak in the HPLC, but growth could be confirmed with colour change and cell growth (Figures 5A and A3). Therefore, organic consumption rates could only be calculated for acetate and lactate.

This experiment confirmed, firstly, that when there is no external CO_2 provided, we do not see any Fe(II) consumption, even when the organics are used. We believe this demonstrates that this strain cannot conduct Fe(II) oxidation with CO_2 from respired organic matter under our experimental conditions. Second, our experiment confirms that growth substrates with a more negative oxidation state than biomass need to have an additional substrate that can serve as an electron sink. In the case of butyrate, this could be CO_2 or substrates like DMSO or protons (resulting in H_2 production) (McKinlay & Harwood, 2010). Gregoire and Poulain successfully demonstrated that mercury (Hg^{II}) could also be used as an electron sink in the purple non-sulphur bacteria *R. capsulatus* SB1003, R.palastris TIE-1 and *Rhodobacter sphaeroides* (Gregoire & Poulain, 2016). This highlights an as yet overlooked role for anoxygenic phototrophs in reducing contaminants as a core facet of their metabolism. It also demonstrates that although CO_2 is the most common electron sink, these bacteria have developed a diversity of strategies to achieve this goal. The environmental importance of using alternative redox-active metals as electron sinks is yet to be widely demonstrated but would be a fruitful avenue of future research. The importance of the oxidation state of the organic compounds was also highlighted in a recent study by Haas et al., 2022, where *R. palustris* CGA010 was tested under nitrogen-fixing, CO_2 absent conditions with Fe(II) and acetate or Fe(II) and malate. Nitrogen fixation

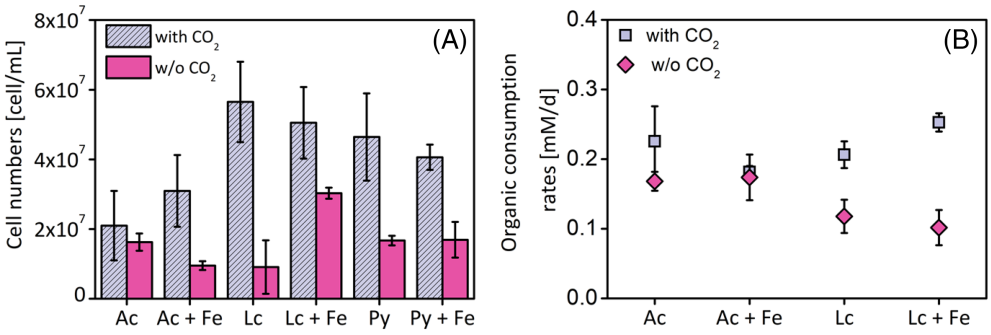

FIGURE 5 (A) Cell numbers of *Rhodopseudomonas palustris* TIE-1 from experiments with CO_2/HCO_3^- (grey striped pattern, with CO_2) or with PIPES buffer (pink coloured bar, w/o CO_2). For organics, results are shown for acetate (Ac), lactate (lc), and pyruvate (Py). Significant changes in cell numbers were calculated for lactate alone and Fe(II) plus pyruvate (Table A1). (B) Organic consumption rates with CO_2/HCO_3^- (grey striped pattern) and with PIPES buffer (pink coloured, w/o CO_2). For lactate alone and Fe(II) plus lactate (Table A1), differences were significant. The standard deviation is based on triplicate measurements.

was used here as an alternative to CO_2 fixation for recycling electron equivalents. No oxidation of Fe(II) was observed with acetate, but when malate, a more oxidised compound, was added, Fe(II) was oxidised. The authors suggest that malate utilisation potentially leads to a more oxidised quinone pool as less flux would go through succinate. This could mean that *R. palustris* TIE-1 could also possibly oxidise Fe(II) without external CO_2 in the presence of a more oxidised substrate like malate.

These results showed that CO_2 is crucial for Fe(II) oxidation and CO_2 produced by oxidation of organic compounds could not serve as a substitute. Fe(II) did not have a notably beneficial effect on organic consumption when PIPES was used as buffer, and the consumption of some organic compounds depend on the co-utilisation of CO_2.

Environmental implications

With these experiments, we demonstrated that Fe(II) oxidation, organic consumption, and the presence of external CO_2 are interdependent, revealing a complex interaction between substrates that dictates growth and Fe(II) oxidation under environmentally relevant conditions. The type of carbon present in the environment can have a marked effect on the contribution of *R. palustris* TIE-1 to Fe(II) oxidation and the contribution of photoferrotrophy to iron cycling. Since both organic compounds and Fe are present in almost all environmental systems in which photoferrotrophs exist, these interactions likely have significant influences on the rates and extent of Fe(II) oxidation, iron mineral formation and organic carbon turnover in the environment.

AUTHOR CONTRIBUTIONS

Verena Nikeleit: Writing – original draft; investigation; methodology; validation; visualization; writing – review and editing; formal analysis; conceptualization; data curation. **Markus Maisch:** Methodology; validation; visualization; writing – review and editing; formal analysis; data curation. **James M. Byrne:** Conceptualization; writing – review and editing; funding acquisition; methodology. **Caroline Harwood:** Conceptualization; writing – review and editing; methodology. **Andreas Kappler:** Conceptualization; writing – review and editing; supervision; resources; project administration; methodology; funding acquisition. **Casey Bryce:** Project administration; conceptualization; funding acquisition; writing – original draft; writing – review and editing; visualization; supervision; resources; methodology.

ACKNOWLEDGEMENTS

The study was supported by Deutsche Forschungsgemeinschaft (DFG, German Research Foundation; BR 5927/2-1 and BY 82/4-1) awarded to C. Bryce and J. M. Byrne. J. M. Byrne is supported by a UKRI Future Leaders Fellowship, MR/V023918/1. The authors gratefully acknowledge the Tübingen Structural Microscopy Core Facility (funded by the Excellence Strategy of the German Federal and State Governments) for their support and assistance in this work. The authors would like to thank Ulf Lüder for laboratory assistance.

CONFLICT OF INTEREST STATEMENT

The authors declare no conflict of interest.

DATA AVAILABILITY STATEMENT

The data that supports the findings of this study are available in the Appendix A of this article.

ORCID

Verena Nikeleit https://orcid.org/0009-0009-9864-4157

Markus Maisch https://orcid.org/0000-0002-4275-4957

James M. Byrne https://orcid.org/0000-0002-4399-7336
Andreas Kappler https://orcid.org/0000-0002-3558-9500
Casey Bryce https://orcid.org/0000-0002-1132-5201

REFERENCES

Bird, L.J., Bonnefoy, V. & Newman, D.K. (2011) Bioenergetic challenges of microbial iron metabolisms. *Trends in Microbiology*, 19(7), 330–340. Available from: https://doi.org/10.1016/J.TIM.2011.05.001

Caiazza, N.C., Lies, D.P. & Newman, D.K. (2007) Phototrophic Fe(II) oxidation promotes organic carbon acquisition by *Rhodobacter capsulatus* SB1003. *Applied and Environmental Microbiology*, 73(19), 6150–6158. Available from: https://doi.org/10.1128/AEM.02830-06

Croal, L.R., Johnson, C.M., Beard, B.L. & Newman, D.K. (2004) Iron isotope fractionation by Fe(II)-oxidizing photoautotrophic bacteria. *Geochimica et Cosmochimica Acta*, 68(6), 1227–1242. Available from: https://doi.org/10.1016/j.gca.2003.09.011

Crowe, S.A., Hahn, A.S., Morgan-Lang, C., Thompson, K.J., Simister, R.L., Llirós, M. et al. (2017) Draft genome sequence of the pelagic photoferrotroph *Chlorobium phaeoferrooxidans*. *Genome Announcements*, 5(13), e01584-16. Available from: https://doi.org/10.1128/GENOMEA.01584-16

Diaz, M.R., Eberli, G.P., Blackwelder, P., Phillips, B. & Swart, P.K. (2017) Microbially mediated organomineralization in the formation of ooids. *Geology*, 45(9), 771–774. Available from: https://doi.org/10.1130/G39159.1

Dohnalkova, A.C., Marshall, M.J., Arey, B.W., Williams, K.H., Buck, E.C. & Fredrickson, J.K. (2011) Imaging hydrated microbial extracellular polymers: comparative analysis by electron microscopy. *Applied and Environmental Microbiology*, 77(4), 1254–1262. Available from: https://doi.org/10.1128/AEM.02001-10

Ehrenreich, A. & Widdel, F. (1994) Anaerobic oxidation of ferrous iron by purple bacteria, a new type of phototrophic metabolism. *Applied and Environmental Microbiology*, 60(12), 4517–4526. Available from: https://doi.org/10.1128/AEM.60.12.4517-4526.1994

Eickhoff, M., Obst, M., Schröder, C., Hitchcock, A.P., Tyliszczak, T., Martinez, R.E. et al. (2014) Nickel partitioning in biogenic and abiogenic ferrihydrite: the influence of silica and implications for ancient environments. *Geochimica et Cosmochimica Acta*, 140, 65–79. Available from: https://doi.org/10.1016/j.gca.2014.05.021

Govindaraju, A., McKinlay, J.B. & LaSarre, B. (2019) Phototrophic lactate utilization by *Rhodopseudomonas palustris* is stimulated by coutilization with additional substrates. *Applied and Environmental Microbiology*, 85(11), e00048-19. Available from: https://doi.org/10.1128/AEM.00048-19

Gregoire, D.S. & Poulain, A.J. (2016) A physiological role for Hg II during phototrophic growth. *Nature Geoscience*, 9(2), 121–125. Available from: https://doi.org/10.1038/ngeo2629

Haas, N.W., Jain, A., Hying, Z., Arif, S.J., Niehaus, T.D., Gralnick, J.A. et al. (2022) PioABC-dependent Fe(II) oxidation during photoheterotrophic growth on an oxidized carbon substrate increases growth yield. *Applied and Environmental Microbiology*, 88(15), e0097422. Available from: https://doi.org/10.1128/aem.00974-22

Han, X., Tomaszewski, E.J., Sorwat, J., Pan, Y., Kappler, A. & Byrne, J.M. (2020) Oxidation of green rust by anoxygenic phototrophic Fe(II)-oxidising bacteria. *Geochemical Perspectives Letters*, 12, 52–57. Available from: https://doi.org/10.7185/geochemlet.2004

Hegler, F., Posth, N.R., Jiang, J. & Kappler, A. (2008) Physiology of phototrophic iron(II)-oxidizing bacteria: implications for modern and ancient environments. *FEMS Microbiology Ecology*, 66(2), 250–260. Available from: https://doi.org/10.1111/j.1574-6941.2008.00592.x

Heising, S., Richter, L., Ludwig, W. & Schink, B. (1999) *Chlorobium ferrooxidans* sp. nov., a phototrophic green sulfur bacterium that oxidizes ferrous iron in coculture with a "*Geospirillum*" sp. strain. *Archives of Microbiology*, 172(2), 116–124. Available from: https://doi.org/10.1007/s002030050748

Heising, S. & Schink, B. (1998) Phototrophic oxidation of ferrous iron by a *Rhodomicrobium vannielii* strain. *Microbiology*, 144, 2263–2269.

Jiao, Y., Kappler, A., Croal, L.R. & Newman, D.K. (2005) Isolation and characterization of a genetically tractable photoautotrophic Fe(II)-oxidizing bacterium, *Rhodopseudomonas palustris* strain TIE-1. *Applied and Environmental Microbiology*, 71, 4487–4496. Available from: https://doi.org/10.1128/AEM.71.8.4487-4496.2005

Kappler, A., Bryce, C., Mansor, M., Lueder, U., Byrne, J.M. & Swanner, E.D. (2021) An evolving view on biogeochemical cycling of iron. *Nature Reviews Microbiology*, 19(6), 360–374. Available from: https://doi.org/10.1038/s41579-020-00502-7

Kappler, A. & Newman, D.K. (2004) Formation of Fe(III)-minerals by Fe(II)-oxidizing photoautotrophic bacteria. *Geochimica et Cosmochimica Acta*, 68(6), 1217–1226. Available from: https://doi.org/10.1016/J.GCA.2003.09.006

Kappler, A., Pasquero, C., Konhauser, K.O. & Newman, D.K. (2005) Deposition of banded iron formations by anoxygenic phototrophic Fe(II)-oxidizing bacteria. *Geology*, 33(11), 865–868. Available from: https://doi.org/10.1130/G21658.1

Konhauser, K.O., Hamade, T., Raiswell, R., Morris, R.C., Ferris, F.G., Southam, G. et al. (2002) Could bacteria have formed the Precambrian banded iron formations? *Geology*, 30(12), 1079–1082. Available from: https://doi.org/10.1130/0091-7613(2002)030<1079:CBHFTP>2.0.CO;2

Kopf, S.H. & Newman, D.K. (2012) Photomixotrophic growth of *Rhodobacter capsulatus* SB1003 on ferrous iron. *Geobiology*, 10(3), 216–222. Available from: https://doi.org/10.1111/j.1472-4669.2011.00313.x

Lambrecht, N., Stevenson, Z., Sheik, C.S., Pronschinske, M.A., Tong, H. & Swanner, E.D. (2021) "Candidatus chlorobium masyuteum," a novel photoferrotrophic green sulfur bacterium enriched from a Ferruginous Meromictic Lake. *Frontiers in Microbiology*, 12(July), 1–17. https://doi.org/10.3389/fmicb.2021.695260

Laufer, K., Niemeyer, A., Nikeleit, V., Halama, M., Byrne, J.M. & Kappler, A. (2017) Physiological characterization of a halotolerant anoxygenic phototrophic Fe(II)-oxidizing green-sulfur bacterium isolated from a marine sediment. *FEMS Microbiology Ecology*, 93(5), fix054. Available from: https://doi.org/10.1093/femsec/fix054

Llirós, M., Garciá-Armisen, T., Darchambeau, F., Morana, C., Triadó-Margarit, X., Inceoğlu, Ö. et al. (2015) Pelagic photoferrotrophy and iron cycling in a modern ferruginous basin. *Scientific Reports*, 5, 13803. Available from: https://doi.org/10.1038/srep13803

McKinlay, J.B. & Harwood, C.S. (2010) Carbon dioxide fixation as a central redox cofactor recycling mechanism in bacteria. *Proceedings of the National Academy of Sciences of the United States of America*, 107(26), 11669–11675. Available from: https://doi.org/10.1073/pnas.1006175107

Melton, E.D., Schmidt, C., Behrens, S., Schink, B. & Kappler, A. (2014) Metabolic flexibility and substrate preference by the Fe(II)-oxidizing purple non-sulphur bacterium rhodopseudomonas palustris strain TIE-1. *Geomicrobiology Journal*, 31(9), 835–843. https://doi.org/10.1080/01490451.2014.901439

Miot, J., Benzerara, K., Obst, M., Kappler, A., Hegler, F., Schädler, S. et al. (2009) Extracellular iron biomineralization by

photoautotrophic iron-oxidizing bacteria. *Applied and Environmental Microbiology*, 75(17), 5586–5591. Available from: https://doi.org/10.1128/AEM.00490-09

Mu, C.C., Zhang, T.J., Zhao, Q., Guo, H., Zhong, W., Su, H. et al. (2016) Soil organic carbon stabilization by iron in permafrost regions of the Qinghai-Tibet Plateau. *Geophysical Research Letters*, 43(19), 10286–10294. Available from: https://doi.org/10.1002/2016GL070071

Nadkarni, M.A., Martin, F.E., Jacques, N.A. & Hunter, N. (2002) Determination of bacterial load by real-time PCR using a broad-range (universal) probe and primers set. *Microbiology*, 148, 257–266.

Patzner, M.S., Mueller, C.W., Malusova, M., Baur, M., Nikeleit, V., Scholten, T. et al. (2020) Iron mineral dissolution releases iron and associated organic carbon during permafrost thaw. *Nature Communications*, 11(6329). https://doi.org/10.1038/s41467-020-20102-6

Peng, C., Bryce, C., Sundman, A., Borch, T. & Kappler, A. (2019) Organic matter complexation promotes Fe(II) oxidation by the photoautotrophic Fe(II)-Oxidizer *Rhodopseudomonas palustris* TIE-1. *ACS Earth and Space Chemistry*, 3(4), 531–536. Available from: https://doi.org/10.1021/acsearthspacechem.9b00024

Poulain, A.J. & Newman, D.K. (2009) *Rhodobacter capsulatus* catalyzes light-dependent Fe(II) oxidation under anaerobic conditions as a potential detoxification mechanism. *Applied and Environmental Microbiology*, 75(21), 6639–6646. Available from: https://doi.org/10.1128/AEM.00054-09

Poulton, S.W. & Canfield, D.E. (2011) Ferruginous conditions: a dominant feature of the ocean through Earth's history. *Elements*, 7(2), 107–112. Available from: https://doi.org/10.2113/gselements.7.2.107

Rancourt, D.G. & Ping, J.Y. (1991) Voigt-based methods for arbitrary-shape static hyperfine parameter distributions in Mössbauer spectroscopy. *Nuclear Instruments and Methods in Physics Research Section B: Beam Interactions with Materials and Atoms*, 58(1), 85–97. Available from: https://doi.org/10.1016/0168-583X(91)95681-3

Solmaz, K.B., Ozcan, Y., Dogan, N.M., Bozkaya, O. & Ide, S. (2018) Characterization and production of extracellular polysaccharides (EPS) by *Bacillus pseudomycoides* U10. *Environments*, 5(6), 63. Available from: https://doi.org/10.3390/environments5060063

Straub, K.L., Rainey, F.A. & Widdel, F. (1999) Marine phototrophic ferrous-iron-oxidizing purple bacteria. *International Journal of Systematic Bacteriology*, 49, 729–735.

Thompson, K.J., Kenward, P.A., Bauer, K.W., Warchola, T., Gauger, T., Martinez, R. et al. (2019) Photoferrotrophy, deposition of banded iron formations, and methane production in Archean oceans. *Science Advances*, 5, eaav2869. Available from: https://doi.org/10.1126/sciadv.aav2869

Tipping, E. (1981) The adsorption of aquatic humic substances by iron oxides. *Geochimica et Cosmochimica Acta*, 45(2), 191–199. Available from: https://doi.org/10.1016/0016-7037(81)90162-9

Widdel, F. (1983) Methods for enrichment and pure culture isolation of filamentous gliding sulfate-reducing bacteria. *Archives of Microbiology*, 134(4), 282–285. Available from: https://doi.org/10.1007/BF00407803

Widdel, F. & Bak, F. (1992) Gram-negative mesophilic sulfate-reducing bacteria. In: Balows, A., Trüper, H.G., Dworkin, M., Harder, W. & Schleifer, K.H. (Eds.) *The prokaryotes*. New York, NY: Springer, pp. 3352–3378. Available from: https://doi.org/10.1007/978-1-4757-2191-1_21

How to cite this article: Nikeleit, V., Maisch, M., Byrne, J.M., Harwood, C., Kappler, A. & Bryce, C. (2024) Phototrophic Fe(II) oxidation by *Rhodopseudomonas palustris* TIE-1 in organic and Fe(II)-rich conditions. *Environmental Microbiology*, 26(3), e16608. Available from: https://doi.org/10.1111/1462-2920.16608

APPENDIX A

TABLE A1 Welsh *t*-test results.

	Setup	*t*	df	*p* Value
Fe(II) oxidation rates with Fe(II) only and Fe(II) plus organics	Acetate	2.86	3.14	.0613
	Lactate	−32.52	4.99	5.30E−07
	Pyruvate	−4.59	4.99	.0059
	Butyrate	No analysis possible		
	Glucose	−3.3	4.12	.0287
Organic consumption rates with Fe and without Fe	Acetate	1.24	2.08	.34
	Lactate	2.92	3.58	.049
	Pyruvate	0.19	2.16	.87
	Butyrate	No analysis possible		
	Glucose	No analysis possible		
Cell numbers with CO_2 and without CO_2	Acetate	0.79	2.37	.5
	Acetate plus Fe	2.91	2.06	.097
	Lactate	5.51	3.84	.0059
	Lactate plus Fe	2.75	2.09	.105
	Pyruvate	4.01	2.07	.0518
	Pyruvate plus Fe	5.33	3.63	.0078
	Butyrate	No analysis possible		
	Glucose	No analysis possible		
Organic consumption rates with CO_2 and without CO_2	Acetate	1.59	2.19	.24
	Acetate plus Fe	0.4	2.27	.73
	Lactate	4.61	4	.01
	Lactate plus Fe	8.75	3.38	.002
	Pyruvate	No analysis possible		
	Butyrate	No analysis possible		
	Glucose	No analysis possible		

Note: Welsh's *t*-test was used to account for unequal variances between each sample treatment. We chose a significance threshold of $\alpha = .05$.

TABLE A2 Calculated and measured cell number of the substrate preference experiment with CO_2.

	Calculated cell number	Measured cell number
Fe(II)	1.2 E+07	2.39 E+07 ± 1.2E+07
Acetate	3.24 E+07	2.10 E+07 ± 8.12E06
Lactate	4.86 E+07	5.6 E+07 ± 1.02E07
Pyruvate	4.86 E+07	4.64 E07 ± 1.02E07
Butyrate	6.48 E+07	6.62 E07 ± 3.07E06
Glucose	9.72 E+07	3.01 E07 ± 2.14E07

Note: For calculations, assumptions were that 90% of electrons from Fe(II) oxidation go into biomass production and 80% of the organics go into biomass.

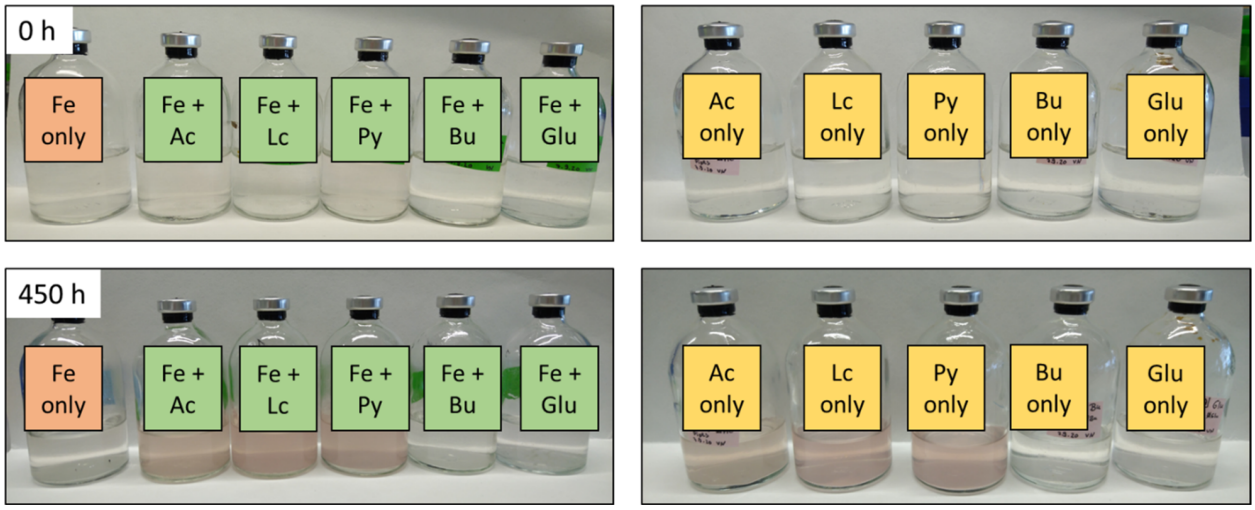

FIGURE A1 PIPES experiment, left side with Fe(II) and organics and on the right side pictures with organics only. Growth can be seen with Fe(II) plus acetate (Ac + Fe), Fe(II) plus lactate (Lc + Fe), Fe(II) plus pyruvate (Py + Fe), and no growth with butyrate (Bu only and Bu + Fe), glucose (Glu only and Glu + Fe) and with Fe only.

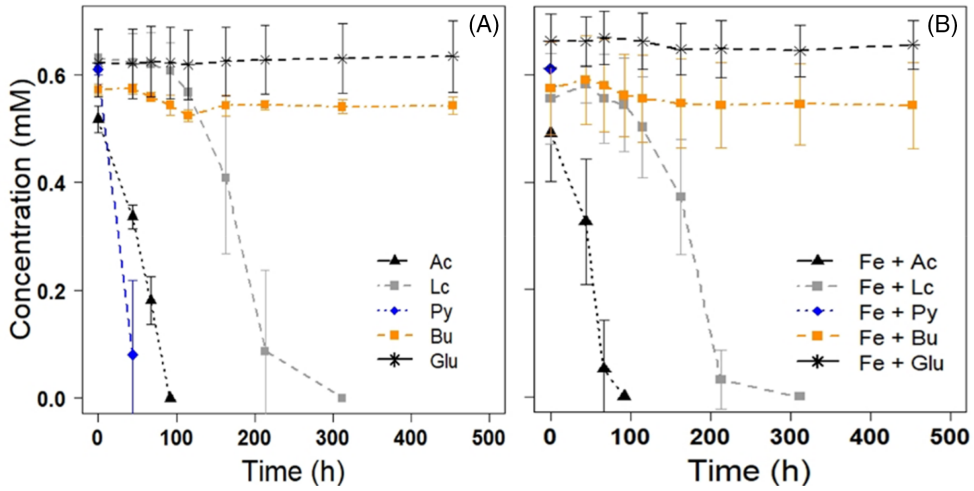

FIGURE A2 Organic consumption over time of *R. palustris* TIE-1 with PIPES buffer. In (A) only organics were added and Ac, Lc and Py were consumed over time. No consumption of Bu and Glu. The same trend could also be observed when Fe(II) was added (B).

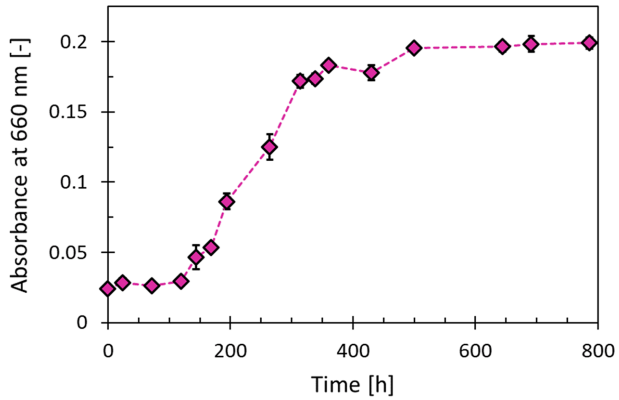

FIGURE A3 *R. palustris* TIE-1 grown in triplicates with glucose and PIPES only.

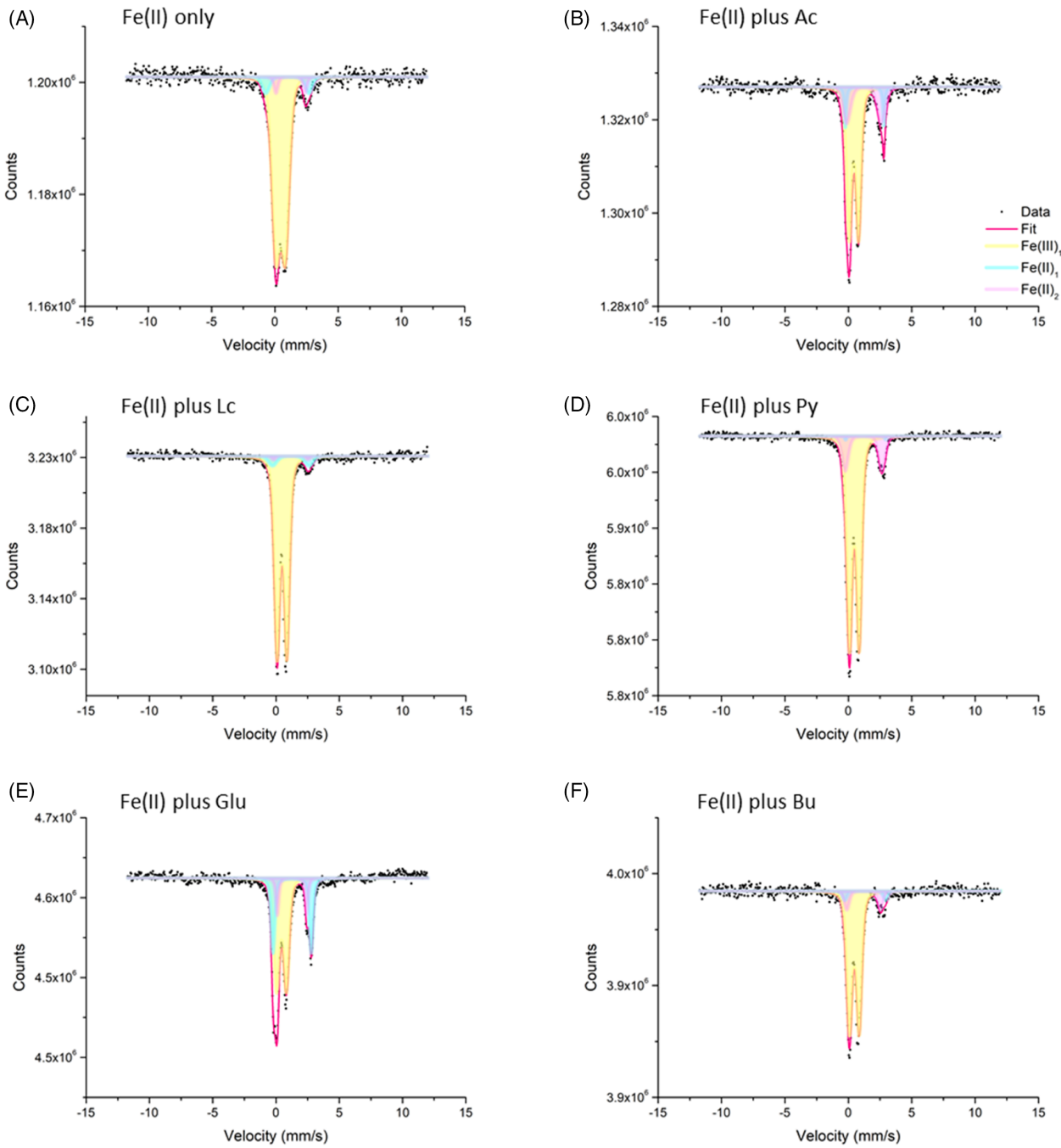

FIGURE A4 Mössbauer spectra collected at 77 K. All samples showed a narrow doublet (Db1; yellow) that can be attributed to the presence of a non-magnetically ordered poorly crystalline Fe(III) mineral phase similar to ferrihydrite. The wide doublet was fitted with two individual doublet features (Db2 and Db3) that can be indicative of Fe(II) mineral phases (Db2; blue) and (Db3; pink) in all samples.

The main components in all samples analyzed differ in their relative abundance. Sample 3f Lactate showed the lowest abundance of Fe(II) mineral phases with <10%. More than 90% of all iron mineral phases detected can be attributed to the presence of ferrihydrite (Table A3). Samples 4f pyruvate and 5f butyrate showed similar Fe(II) mineral abundances of around 15%, while ferrihydrite represented approximately 85% of the abundant iron mineral phases. The highest relative abundance of Fe(II) mineral phases was detected in samples 1f and 2f with about 30%–45% Fe(II) being present. Ferrihydrite showed a lower relative abundance in these samples compared to the previous ones, reaching a relative abundance of 50%–70% only.

TABLE A3 Overview of Mössbauer spectra fitting parameters.

Sample	Temp. (K)	Phase	CS (mm/s)	ΔE_Q (mm/s)	Pop (%)	χ^2	Mineral phase
TIE-1 Fe(II) only	77	Db1	0.48	0.80	87.5	0.64	Fe(III)
		Db2	1.00	3.21	7.7		$Fe(II)_1$
		Db3	1.24	2.30	4.8		$Fe(II)_2$
TIE-1 Fe(II) plus acetate	77	Db1	0.48	0.74	68.3	0.69	Fe(III)
		Db2	1.38	3.05	23.1		$Fe(II)_1$
		Db3	1.10	2.83	8.6		$Fe(II)_2$
TIE-1 Fe(II) plus lactate	77	Db1	0.48	0.77	94.4	0.69	Fe(III)
		Db2	1.18	3.16	3.5		$Fe(II)_1$
		Db3	1.13	2.72	2.1		$Fe(II)_2$
TIE-1 Fe(II) plus pyruvate	77	Db1	0.48	0.76	84.9	1.38	Fe(III)
		Db2	1.37	3.16	6.6		$Fe(II)_1$
		Db3	1.20	2.92	8.5		$Fe(II)_2$
TIE-1 Fe(II) plus butyrate	77	Db1	0.48	0.76	86.0	0.71	Fe(III)
		Db2	1.34	3.21	7.7		$Fe(II)_1$
		Db3	1.21	2.66	6.3		$Fe(II)_2$
TIE-1 Fe(II) plus glucose	77	Db1	0.43	0.78	59.3	0.73	Fe(III)
		Db2	1.28	3.01	28.9		$Fe(II)_1$
		Db3	1.27	2.32	11.8		$Fe(II)_2$

Note: Temp., temperature during measurement; Phase, fitted compound; Db, doublet, center shift (CS in mm/s); quadrupole splitting (ΔE_Q in mm/s); quadrupole shift (ε in mm/s); hyperfine field (B_{hf} in T); Pop, relative abundance (in %), χ^2 as goodness of fit and identified iron speciation/mineral phase: Fe(III) most likely ferrihydrite, $Fe(II)_1$ and $Fe(II)_2$ as ferrous iron mineral phases.

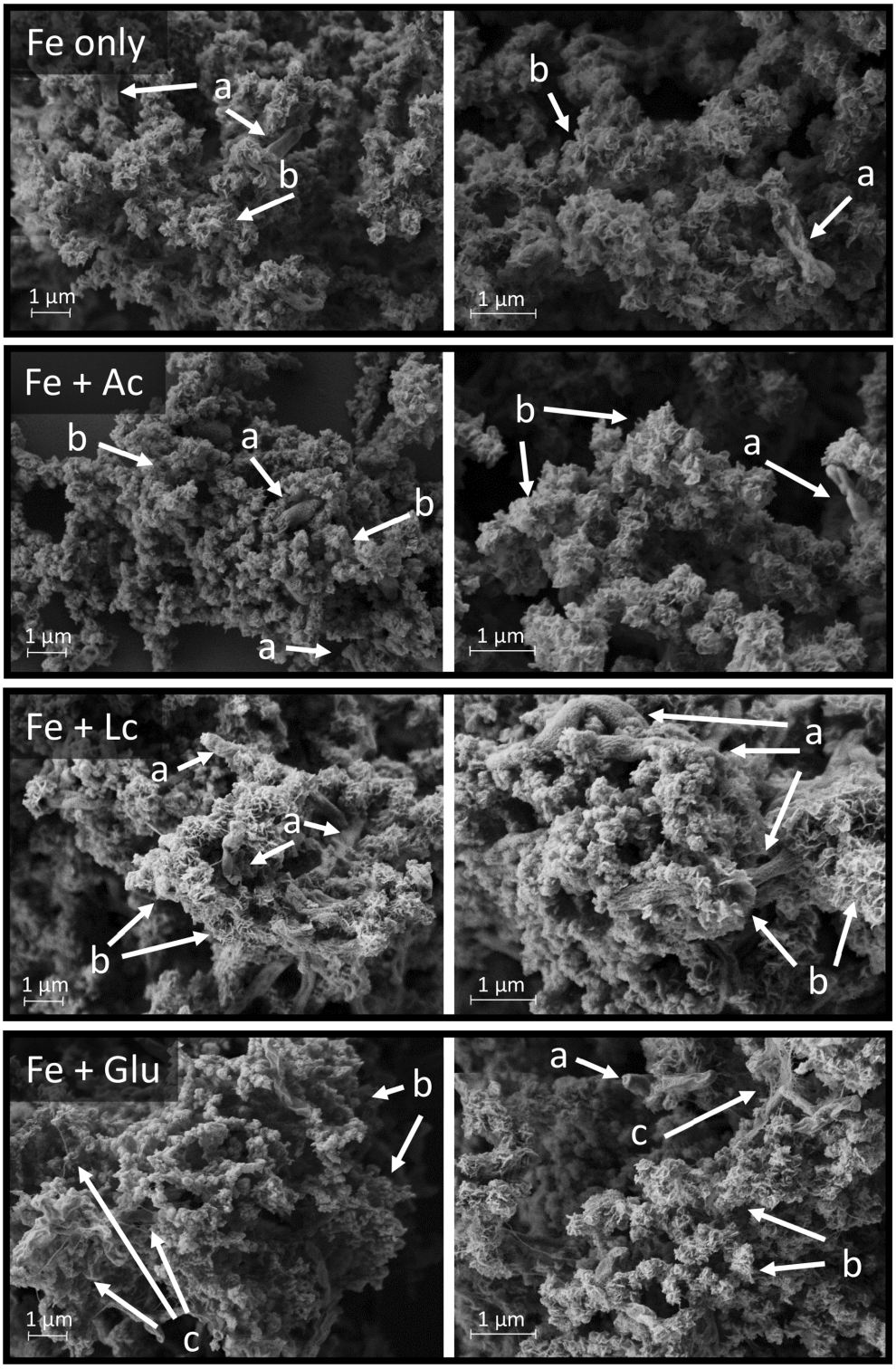

FIGURE A5 SEM images of *R. palustris* TIE-1 grown with only Fe(II) (Fe only), with Fe(II) plus acetate (Fe + Ac), with Fe(II) plus lactate (Fe + Lc) and with Fe(II) plus glucose (Fe + Glu). Arrow a shows the cells of *R. palustris* TIE-1, arrow b shows the spiky minerals and arrow c shows spider-web-like structures.